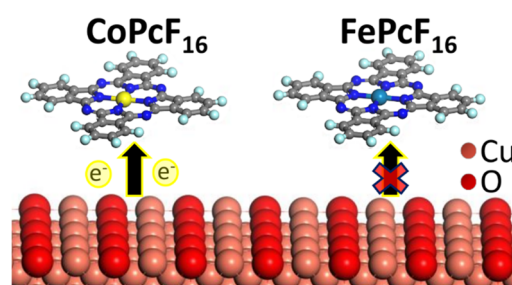


Perfluorinated Phthalocyanines on Cu(110) and Cu(110)-(2 × 1)O: The Special Role of the Central Cobalt Atom

Axel Belser, Katharina Greulich, Peter Grüninger, Reimer Karstens, Ruslan Ovsyannikov, Erika Giangrisostomi, Peter Nagel, Michael Merz, Stefan Schuppler, Thomas Chassé, and Heiko Peisert*

ABSTRACT: Interface properties of CoPcF₁₆ on Cu(110) and Cu(110) (2 × 1)O were investigated by X ray photoemission spectroscopy (XPS), ultraviolet photoemission spectroscopy (UPS), X ray absorption spectroscopy (XAS), and scanning tunneling microscopy (STM). The results are compared to FePcF₁₆ on Cu(110) (2 × 1)O. A charge transfer from both substrates to the central Co ion of CoPcF₁₆ is observed. Unlike to FePcF₁₆ and related molecules, the strong interaction between CoPcF₁₆ molecules of the first layer and the Cu(110) substrate is only partially suppressed by oxygen termination. The special nature of the electronic structure of the Co ion in Co phthalocyanines is discussed. The analysis of the fluorine Auger parameter enables the discussion of initial and final state effects of core level binding energy shifts in photoemission. A bidirectional charge transfer also involving the macrocycle of CoPcF₁₆ molecules is concluded.



1. INTRODUCTION

The tuning of electronic interface properties between organic molecules and metallic substrates is of enormous importance for a broad variety of applications.^{1–3} Strong interactions including chemical reactions may especially alter the molecular electronic structure of the frontier orbitals, which are important for charge carrier transport and injection. Routes to avoid chemical interactions at interfaces include, among others, the optimization of the surface preparation or the introduction of intermediate layers.^{4–9} Copper surfaces are among the more reactive substrates, where a strong chemisorption is observed for many organic molecules.^{9–17} For some systems, such interactions can be avoided by an oxygen termination of the copper surface.^{16,18}

The interface properties of cobalt phthalocyanine (CoPc) seem to be different compared to other transition metal phthalocyanines: In many cases, interaction at the interfaces between CoPcF_X (X = 0, 16) and noble metals is governed by a local interaction between the Co 3d_{z²} orbital and states of the metal substrate,^{19,20} and a charge donation was observed for many interfaces (e.g., refs 19–22). In this study, we compare interface properties of CoPcF₁₆ on Cu(110) and Cu(110) (2 × 1)O. To assess the special role of the central Co ion, the results are compared to FePcF₁₆ on Cu(110) (2 × 1)O.

2. EXPERIMENTAL SECTION

The Cu(110) single crystal was cleaned by several cycles of Ar⁺ ion sputtering and subsequent annealing. The sputtering was performed at a voltage of 1.0 kV for typically 30 min at an argon partial pressure of 5 × 10⁻⁵ mbar, and the annealing was

performed for 30 min at a temperature of 750 K. The crystal cleanliness and orientation were checked by X ray photo emission spectroscopy (XPS), low energy electron diffraction (LEED), and scanning tunneling microscopy (STM). The Cu(110) (2 × 1)O surface was prepared by exposing the clean surface to 20 langmuirs of oxygen at room temperature, followed by heating to 570 K for 4 min.

CoPcF₁₆ (Sigma Aldrich) and FePcF₁₆ (SYNTHON Chemicals GmbH & Co. KG) powders were evaporated at rates of 0.2–0.4 nm/min and a temperature of 650–670 K from a temperature controlled crucible. The evaporation rates were estimated from a quartz microbalance. The nominal film thickness was estimated from XPS intensity ratios by using sensitivity factors from Yeh and Lindau²³ assuming layer by layer growth for each deposition step.

The photoemission measurements (XPS and ultraviolet photoemission spectroscopy (UPS)) were performed in the home lab by using a multichamber UHV system (base pressure of 2 × 10⁻¹⁰ mbar) equipped with a Phoibos 150 hemispherical energy analyzer (SPECS), an X ray source with monochromator (XR 50 M, SPECS), and a helium discharge lamp (SPECS). The energy resolution for XPS (excitation energy $h\nu = 1486.7$ eV) and UPS ($h\nu = 21.22$ eV) was 400 and

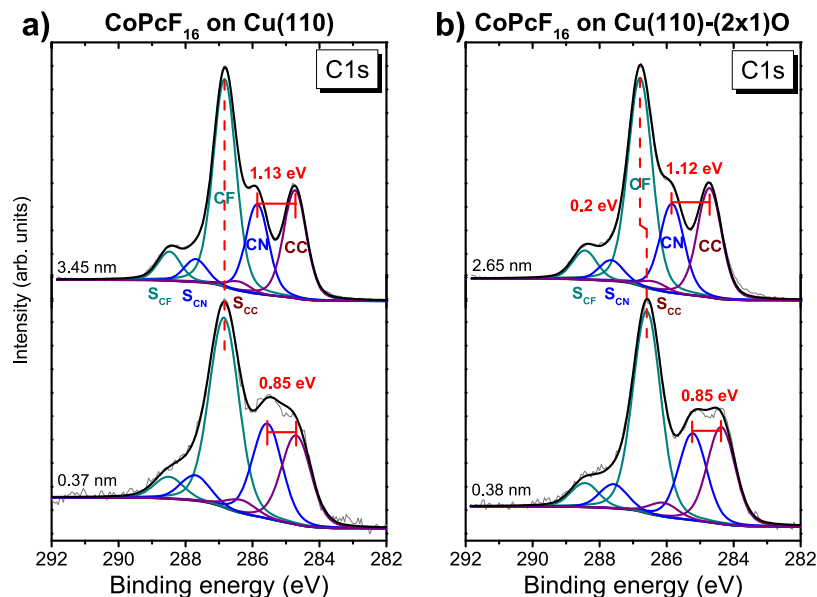


Figure 1. Thickness dependent C 1s core level spectra for CoPcF₁₆ on (a) Cu(110) and (b) Cu(110) (2 × 1)O. Except for minor differences in the relative energy position of the components, the same model can be applied for the description of all spectra.

Table 1. CoPcF₁₆ on Cu(110) and Cu(110) (2 × 1)O: Thickness Dependent C 1s Binding Energies as Obtained from Peak Fits in eV

substrate	thickness (nm)	CF	SCF	CN	SCN	CC	SCC
Cu(110)	3.45	286.83	288.48	285.86	287.70	284.73	286.42
	0.37	286.85	288.50	285.55	287.72	284.70	286.35
Cu(110)-(2 × 1)O	2.65	286.79	288.44	285.84	287.66	284.72	286.38
	0.38	286.59	288.44	285.22	287.59	284.37	286.09

150 meV, respectively. The binding energy was calibrated with respect to the Au 4f_{7/2} (84.0 eV) and the Cu 2p_{3/2} (932.6 eV) peak positions. The peak fitting of XP spectra was performed by using the program Unifit.²⁴ A Voigt profile peak shape (convolution of Gaussian and Lorentzian peaks) and a Shirley model background were used.

The corresponding X ray absorption spectroscopy (XAS) measurements of the NK and Co L edges have been performed at the PM4 beamline (LowDose PES endstation) at BESSY II (Helmholtz Zentrum Berlin, Germany) and the measurements of the Fe L edge at the WERA beamline at the Karlsruhe Research Accelerator (KARA, Karlsruhe, Germany). The energy resolution at the PM4 beamline was set at 100 meV at a photon energy of 400 eV and at the WERA beamline at 220 and 340 meV at photon energies of 400 and 710 eV. The XA spectra at both beamlines were monitored indirectly by measuring the total electron yield (sample current).

The STM measurements were performed in a two chamber UHV system equipped with a low energy electron diffraction (LEED) system from OCI Vacuum Microengineering Inc. and a variable temperature (VT) STM from Omicrometer GmbH. For the STM measurements, mechanically cut Pt/Ir tips were used. All given tunneling voltages are referenced to the sample. The WSxM program was used to tune the image contrast.²⁵

3. RESULTS AND DISCUSSION

3.1. Interaction between the CoPcF₁₆ Macrocycle and the Substrates. Different interaction channels are observed between phthalocyanines and a variety of substrates, involving both the macrocycle and the central metal atom; often the

charge transfer is bidirectional.^{15,26–28} First, we will discuss interactions between the CoPcF₁₆ macrocycle (i.e., the C and N atoms) and the copper substrates.

In Figure 1, we show C 1s core level spectra for CoPcF₁₆ on Cu(110) and Cu(110) (2 × 1)O at about one monolayer coverage (0.37 nm) compared to bulklike thin films. 0.32 nm corresponds to one monolayer of flat lying perfluorinated phthalocyanines, as can be inferred from the crystal structure.²⁹ Data for additional thicknesses are provided as Supporting Information (Figure S1). As for related perfluorinated phthalocyanines,^{15,30} the C 1s core level spectra for the bulklike, thickest films can be fitted by using three main components in sequential order from high to low binding energy: carbon bonded to fluorine (CF), bonded to nitrogen (CN), and bonded to other carbon (CC). All main peaks are accompanied by their respective satellites, denoted S_{CF}, S_{CN}, and S_{CC} in Figure 1. The intensity ratio estimated from the peak areas CF:CN:CC (including related satellites) of 4:1.9:2 is in reasonable agreement with the stoichiometric composition (4:2:2). Energetic positions obtained from the peak fits shown in Figure 1 are summarized in Table 1.

Essentially the same model can be applied for the description of the spectra for low coverages of about 0.37 nm. The intensity ratio CF:CN:CC agrees well with the expectation according to stoichiometry: 4:2.3:1.9 and 4:2:2 for Cu(110) and Cu(110) (2 × 1)O, respectively. The energetic position of satellites with respect to the main lines as well as the Lorentzian widths (0.2 eV) were kept constant. Generally higher Gaussian widths were obtained for the low coverages (about 0.9 eV; thicker films: about 0.7 eV), which might be

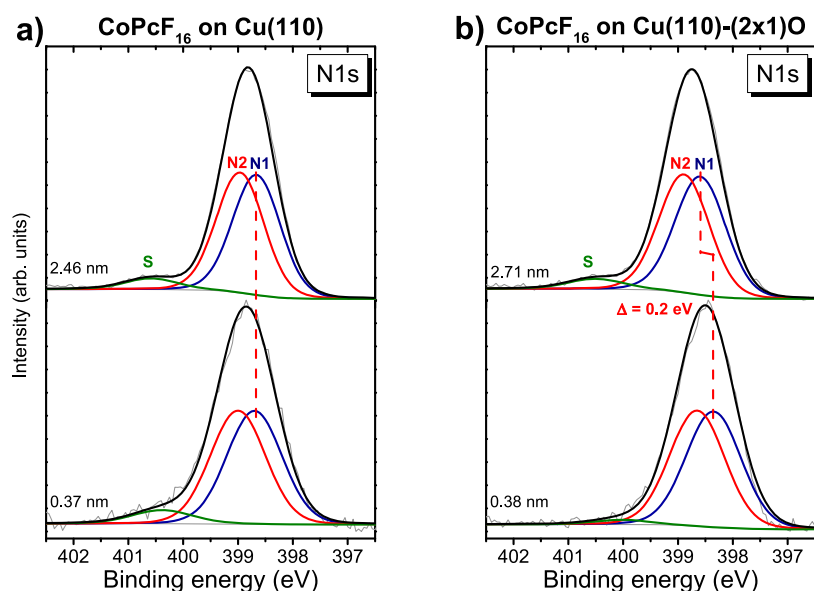


Figure 2. Thickness dependent N 1s core level spectra for CoPcF₁₆ on (a) Cu(110) and (b) Cu(110) (2 × 1)O.

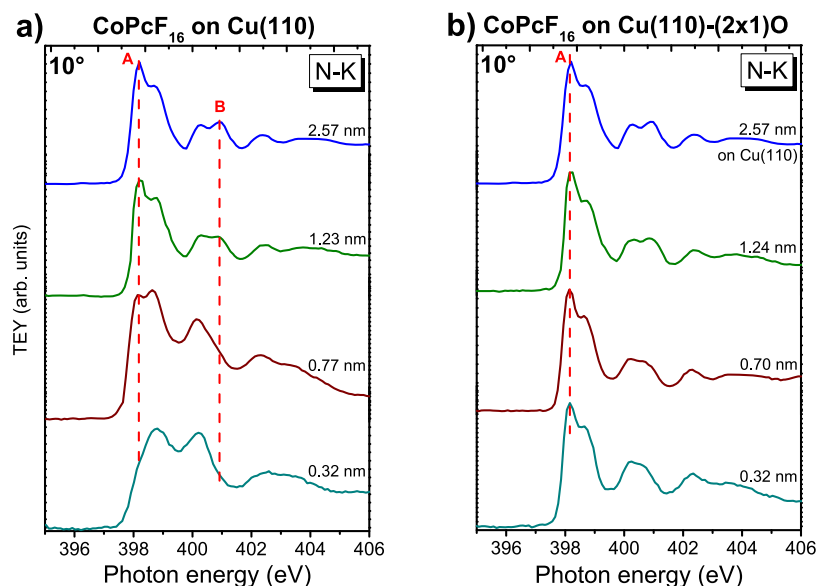


Figure 3. Thickness dependent N 1s excitation spectra at grazing incidence (10°) for CoPcF₁₆ on (a) Cu(110) and (b) Cu(110) (2 × 1)O. The reference for the bulklike spectrum of the thickest film in (b) is taken from (a). Because of a complex background treatment, the exact determination of the step height is complicated.

ascribed to adsorption at inequivalent adsorption sites or another kind of disorder, which may cause a statistical distribution of orbital energies.³¹

However, the detailed analysis of energetic positions of the C 1s components in Figure 1 (cf. Table 1) reveals distinct differences between monolayer coverages and thicker films. Generally, in close proximity to metallic substrates, a shift of core level binding energies to lower values is expected due to final state screening effects of the photohole as the additional mirror charge screening. Such energetic shifts are often in the range 0.3–0.6 eV.^{32–35} For the investigated samples these effects may affect the observed binding energies. However, additional effects must influence the observed energetic positions because the peak components are not shifted by equal amounts. Most visible in Figure 1, the distance between CC and CN is decreased by more than 0.25 eV for molecules

directly at the interface (monolayer coverage), compared to thicker films, similar to FePcF₁₆ on Cu(111).¹⁵ A possible reason might be a site dependent screening or a redistribution of electrons for molecules of the first layer on both substrates.³⁶ The stronger shift of CN to lower binding energies compared to CC at the interface would imply a relative increase of electron density at the CN atoms of the interface layer.

Also, N 1s spectra, shown in Figure 2, exhibit almost no thickness dependent changes of the peak shape (complete series shown in Figure S2). The main line consists of two signals of the same intensity for the pyrrole and the bridging nitrogen atoms, denoted N1 and N2 in Figure 2. Because their energy separation is small for related phthalocyanines (0.3–0.5 eV),^{37–42} they cannot be clearly resolved by XPS. Peak fit parameters are given as Supporting Information (Table

S1). Similar to C 1s (cf. Figure 1), all N 1s spectra can be fitted by using the same model, independent of the layer thickness. Only the Gaussian width is slightly increased for low coverages (by about 0.1 eV), most likely due to adsorption at inequivalent sites of the substrate surface (cf. discussion of the C 1s peak shape). Similar to C 1s, peak shifts to lower binding energy are observed for low coverages CoPcF₁₆ on Cu(110) (2 × 1)O, most likely due to screening effects.

The corresponding N 1s XA spectra taken at grazing incidence are shown in Figure 3. The CoPcF₁₆ molecules grow in a preferred flat lying adsorption geometry, as concluded from the angular (polarization) dependence of N K XA spectra at higher film thicknesses (see Figure S3). Thus, at the chosen measurement geometry, features below 404 eV arise predominantly from transitions into π^* molecular orbitals. For phthalocyanines, most intense π^* resonances (denoted A) are assigned to transitions from N 1s to LUMO e_g orbitals.^{43,44} The complex structure of feature A arises from an involvement of the ligand LUMO in the hybridization with the central metal atom of the Pc.^{42,43,45–49}

It was shown that π^* resonances in N K edge absorption spectra are very sensitive on involvement of nitrogen in the interfacial interactions.^{20,45,50,51} Indeed, for CoPcF₁₆ on Cu(110) distinct changes of the peak shape as a function of the film thickness are visible in Figure 3a. The ratio between the intensities of features A and B at photon energies of 398.2 and 400.9 eV decreases for lower coverages, reminiscent of FePcF₁₆ on Cu(111) or FePc on Ag(111).^{15,50} This may indicate (partial) charge transfer from the Cu(110) substrate to the (ligand) LUMO of CoPcF₁₆. Because the corresponding N 1s core level photoemission spectra are almost unaffected by the interface interaction, the charge transfer may occur into the (delocalized) LUMO; in other words, the electron density is not (only) localized at the nitrogen atoms. In contrast to the Cu(110) substrate, for CoPcF₁₆ on Cu(110) (2 × 1)O (Figure 4b), the peak shape is almost the same for all thicknesses, indicating that nitrogen is not involved in the interaction at the interface.

A localized, strong interaction between nitrogen and the Cu(110) substrate may result in the breaking of chemical

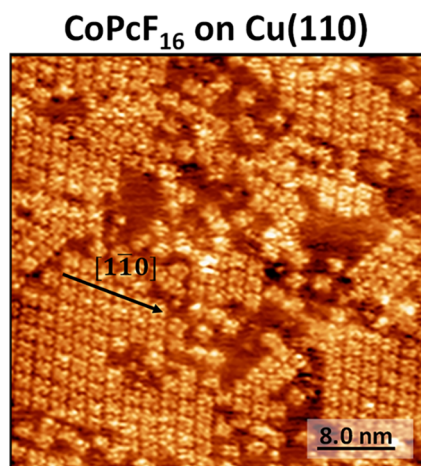


Figure 4. STM image of a submonolayer coverage of CoPcF₁₆ on Cu(110) (about 0.7 ML). The 4 fold symmetry of the molecules is typical for phthalocyanines, indicating that the molecules remain intact upon adsorption on Cu(110). Measurement parameters: $I = 300$ pA and $U = 0.7$ V.

bonds within the macrocycle of CoPcF₁₆. To further investigate the interface interaction in more detail, we performed STM measurements for the apparently most reactive interface CoPcF₁₆/Cu(110). In Figure 4, an STM image of a CoPcF₁₆ submonolayer is shown. Clearly, the typical 4 fold symmetry of the phthalocyanine molecules can be identified. Similar to CoPcF₁₆ on Ag(110),⁵² the molecules are aligned along the $[1\bar{1}0]$ direction of the substrate. Thus, we conclude that the CoPcF₁₆ molecules appear intact upon adsorption on the Cu(110) surface.

3.2. Interactions between the Central Metal Atom of the Phthalocyanines and the Substrates. For transition metal phthalocyanines, the study of both 2p photoemission and X ray absorption spectroscopy yields valuable information about the electronic structure of the central metal atom at interfaces. In Figure 5, we show Co 2p_{3/2} core level photoemission for CoPcF₁₆ on Cu(110) (Figure 5a) and on Cu(110) (2 × 1)O (Figure 5b) as a function of thickness. On both substrates the spectrum of the thickest layer shows the typical multiplet structure, as known for Co phthalocyanines.^{26,40,53,54} Clearly visible, with decreasing layer thickness an additional (interface) peak at lower binding energy develops, located at 778.4 and 778.1 eV for CoPcF₁₆ on Cu(110) and Cu(110) (2 × 1)O, respectively. The lower binding energy compared to the main component implies a higher electron density or, in other words, a reduction of the Co²⁺ ion at the interface. The different binding energy on both substrates is most likely caused by a different energy level alignment of the first layer. Thus, a charge transfer from the substrate to the central metal atom of the phthalocyanine occurs on both substrates, similar to CoPcF₁₆ on other metals.^{5,26,53}

Also visible in Figure 5, the intensity of the interface component is clearly different for the about monolayer coverages (0.37 and 0.38 nm) on the two substrates. On the Cu(110) substrate (Figure 5a), the shape of the spectrum is typical for reduced Co at reactive metal substrates;^{26,27,53,55} the intensity at binding energies >780 eV can be assigned to satellite (i.e., multiplet) structures.⁴⁰ In contrast, for the same CoPcF₁₆ coverage on Cu(110) (2 × 1)O (Figure 5b), the relative intensity at binding energies >780 eV is distinctly increased, indicating remaining intensity from the Co²⁺ multiplet, which is similar to CoPcF₁₆ at a copper intercalated graphene/Ni(111) interface.⁵ Thus, it seems that not all molecules of the first monolayer on Cu(110) (2 × 1)O undergo a charge transfer; apparently the interaction strength depends crucially on the adsorption site. The importance of different adsorption sites has been shown in detail for other large organic molecules as, for example, 4' (4 tolyl) 2,2':6',2'' terpyridine on Au(111).⁵⁶

Additional information about the (unoccupied) electronic structure of the central metal atom can be gained from the corresponding Co 2p excitation spectra. Thickness dependent Co L₃ edge XA spectra of CoPcF₁₆ on both substrates are shown in Figure 6 for grazing (10°) and normal (90°) incidence of the incoming linearly polarized synchrotron light. The angular dependence can be understood by polarization rules for transitions into different orbitals. For the almost flat lying molecules (cf. discussion of the angular dependence of N K XA spectra, Figure S3), transitions into orbitals with out of plane components (e.g., d_{z²}) are strongest at grazing incidence, while at normal incidence transitions into orbitals with in plane components (d_{x²-y²} and d_{xy}) are most intense. For a detailed

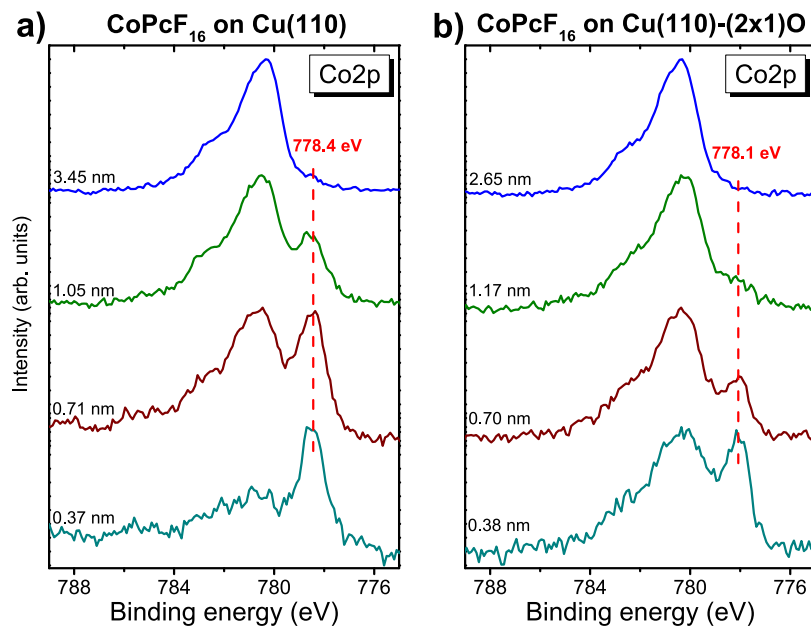


Figure 5. Thickness dependent Co $2p_{3/2}$ core level spectra for CoPcF₁₆ on (a) Cu(110) and (b) Cu(110) (2×1)O.

discussion of the spectral shape, see refs 5, 57, and 58. Out of plane transitions are labeled with “A”, while in plane transitions are labeled with “B” in Figure 6. The spectra for the thickest, bulklike film of 2.57 nm are typical for flat lying CoPc or CoPcF₁₆ molecules on different substrates.^{5,20,57} However, for lower coverages the peak shape of Co 2p excitation spectra changes distinctly. While the feature A dominates the bulklike spectra at grazing incidence, a new feature, denoted A0, appears for lower coverages in Figure 6a,b. Such a feature A0 was observed for CoPc on other reactive substrates, such as Ag or Ni, and can be understood by a hybridization of the Co d_{z^2} orbital with substrate related orbitals.^{20,59} At the same time, at normal incidence feature B2 disappears for low coverages (Figure 6c,d), indicating that the charge transfer is accompanied by a redistribution of the d electrons at the central metal atom of the phthalocyanine at the interface.²⁰

Comparing the Co L_3 edge XA spectra for monolayer coverages in Figure 6, it becomes evident that the shape distinctly depends on the substrate. Feature A0 completely dominates the spectrum at grazing incidence on Cu(110), whereas A is still the most intense feature on Cu(110) (2×1)O. At normal incidence, feature B2 disappears on Cu(110), while it is still visible on Cu(110) (2×1)O. The behavior indicates that for a portion of the molecules of the first layer on Cu(110) (2×1)O no charge transfer occurs at the interface.

Thus, both 2p photoemission and excitation spectra reveal that the oxygen termination of the Cu(110) (2×1)O substrate prevents the interfacial charge transfer to the Co²⁺ ion only partly. This is somewhat surprising, since for even smaller molecules like hexacene,¹⁸ an almost complete electronic decoupling by the oxygen rows is observed. The one dimensional Cu–O rows, aligned along the [001] direction of the Cu(110) surface, have a distance of about 0.51 nm, i.e., distinctly smaller than the size of CoPc or CoPcF₁₆ molecules. For details of the Cu(110) (2×1)O reconstruction, see Figures S7 and S8 and refs 60–62. Thus, one might conclude that the charge transfer occurs between atoms of the Cu–O rows and the Co ion of the phthalocyanine.

The different behavior of CoPcF₁₆ compared to other molecules might be the special nature of the half filled d_{z^2} orbital of the Co ion of Co phthalocyanines, which is oriented toward the substrate for flat lying molecules. Recent experimental and theoretical works demonstrate that charge transfer occurs from the formation of a molecule–metal hybrid state, which is most likely due to a local bond between the Co $3d_{z^2}$ orbital and metal states.^{19,53,55,63,64} In addition, the observation of similar interface interactions for cobalt octaethylporphyrin and cobalt tetraphenylporphyrin on different substrates suggests they are almost independent of the ligand or macrocycle.^{65–67}

To study the particular role of the central Co ion in CoPcF₁₆ for interface interactions, we compare our results to FePcF₁₆ on Cu(110) (2×1)O. Fe 2p XP spectra and Fe L_3 edge XA spectra for FePcF₁₆ on Cu(110) (2×1)O as a function of the film thicknesses are shown in Figure 7. For a detailed discussion of the peak shape, we refer to the literature on FePc and FePcF₁₆.^{20,43,47,51,68,69} Although most literature confirms for Fe²⁺ in FePc a 3E_g ground state with a configuration $(b_{2g})^2(e_g)^3(a_{1g})^1$, the electronic configuration is much more flexible compared to Co²⁺ in Co phthalocyanines.^{70–72}

The Fe 2p XP spectrum of a multilayer (0.83 nm) in Figure 7a exhibits a broad multiplet structure; similar spectra were reported for both FePc and FePcF₁₆.^{50,51,68} Most important, no interface component can be detected in the related monolayer spectrum, which might be expected at about 707 eV (compare, e.g., FePc on Ag(111)⁵⁰ and FePcF₁₆ on Cu(111)¹⁵). Also, the peak shape of the corresponding XA spectra is almost independent of the film thickness; differences may also arise from artifacts due to the complex background subtraction procedure. For example, a feature similar to “A0” observed on Cu(110) (Figure 6a) and related reactive interfaces^{15,50} at grazing incidence of the incoming p polarized synchrotron light is not detectable.

Therefore, we conclude that the first monolayer of FePcF₁₆ is widely decoupled from the Cu(110) (2×1)O substrate surface. There is no evidence for a substantial charge transfer

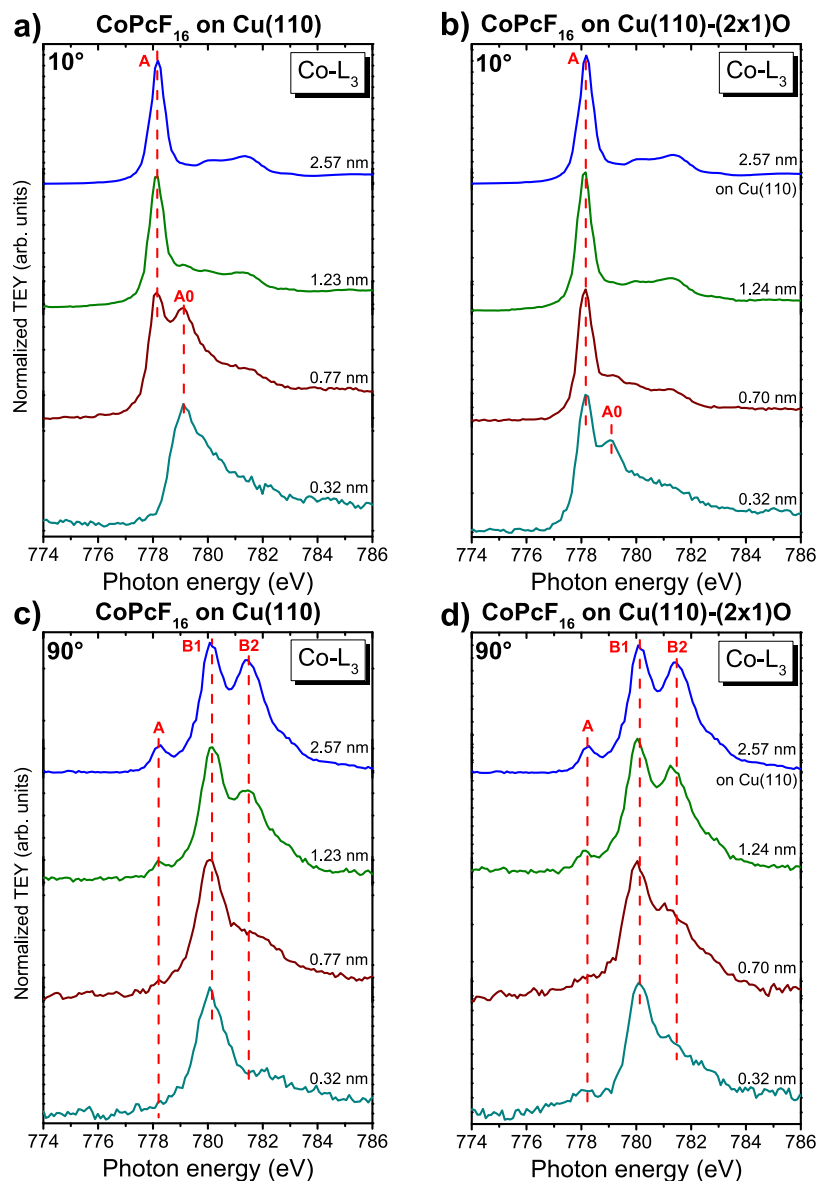


Figure 6. Thickness dependent Co 2p excitation spectra at grazing incidence (10°) for CoPcF₁₆ on (a) Cu(110) and (b) Cu(110) (2×1)O and normal incidence (90°) for CoPcF₁₆ on (c) Cu(110) and (d) Cu(110) (2×1)O.

to the Fe²⁺ ion. The result is in good agreement with studies of FePc on Cu(110) and Cu(110) (2×1)O, where a switching of the spin state of the central Fe ion was observed on the strongly interacting Cu(110) substrate, while such spin switching is absent on the oxygen terminated Cu(110) (2×1)O with weak or negligible interactions.¹⁶ As a consequence, we are left with the conclusion that the special electronic configuration of the Co ion in CoPcF₁₆ triggers the charge transfer at some adsorption sites on Cu(110) (2×1)O.

3.3. Total Interfacial Charge Transfer and Valence Electronic Structure. So far, evidence for a rather local charge transfer from both substrates to the Co ion of CoPcF₁₆ was provided. In addition, for the Cu(110) substrate, also a charge transfer to the LUMO of CoPcF₁₆ was discussed. As a consequence of such charge transfer, dipoles at the interface are formed, which can be quantitatively determined by UPS (for details, see Figure S4).

In Figure 8, the energy level alignment for CoPcF₁₆ on Cu(110) and Cu(110) (2×1)O is summarized. In first

approximation, the ionization potential (IP) can be regarded as a property of the material, although it was shown that presence of an intrinsic surface dipole may result in distinctly different values of the IP in highly ordered assemblies with differently oriented molecules.^{73,74} The measured ionization potentials of CoPcF₁₆ in thin films (6.19 and 6.12 eV in Figure 8) are typical for fluorinated phthalocyanines and in good agreement with the literature.⁵ The high IP supports charge transfer to the molecule on substrates with comparably low work function.⁵ Indeed, large interface dipoles are observed on both substrates in Figure 8, indicating a total charge transfer from the substrate to the molecule. We note that not only interfacial charge transfer causes the formation of interface dipoles, an important effect is the modification of the substrate work function upon adsorption of molecules (push back effect).^{32,75,76} However, for many systems values for a push back effect in the order of 0.3–0.6 eV were found,^{32,34,77} which is distinctly lower than dipoles determined in Figure 8.

FePcF₁₆ on Cu(110)-(2x1)O

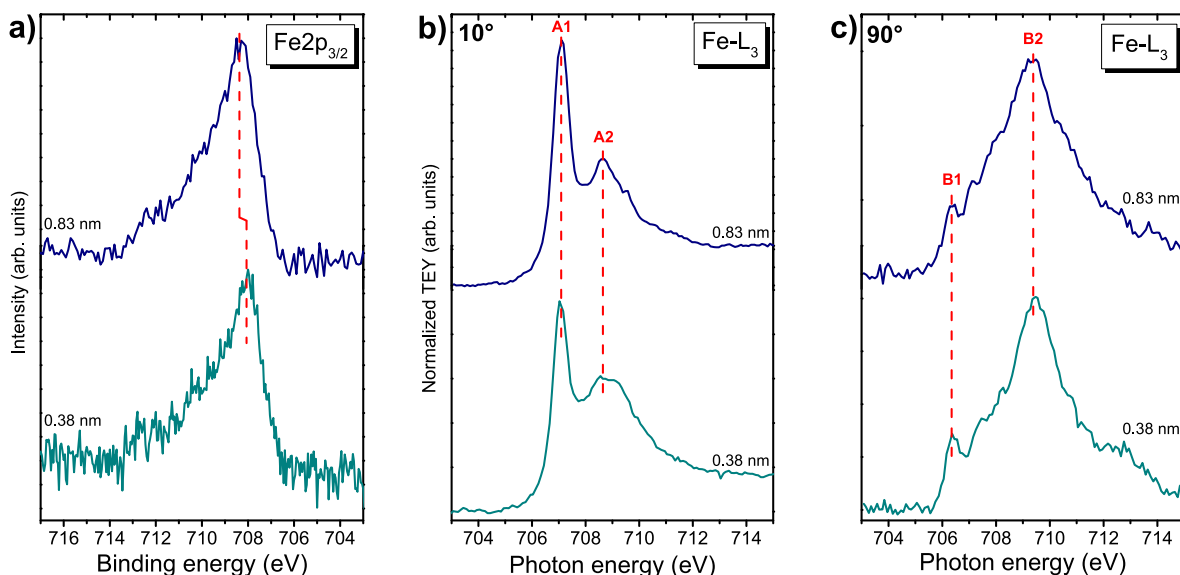


Figure 7. Thickness dependent FePcF₁₆ on Cu(110) (2 × 1)O. (a) Fe 2p_{3/2} core level spectra, (b) X ray absorption spectra at grazing incidence (10°), and (c) X ray absorption spectra at normal incidence (90°).

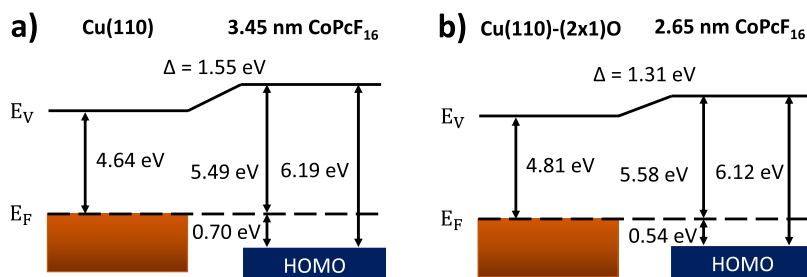


Figure 8. Energy level alignment of CoPcF₁₆ on (a) Cu(110) and (b) Cu(110) (2 × 1)O. In both cases, the large dipoles indicate a total charge transfer from the substrate to the molecule.

The question may arise whether the charge transfer occurs unidirectionally from the substrate to the molecule or whether the interaction is bidirectional, as observed for related interfaces.^{15,26–28} To discuss a possible charge transfer from the macrocycle to the substrate in more detail, we come back to the core level shifts, observed in section 3.1. Generally, such shifts can be caused by initial state effects (i.e., a different local electron density) or final state effects as a response to the formation of the photohole (screening).^{36,78–80} Whereas the screening causes a lowering of the binding energy, an opposite effect is expected by an electron transfer from the molecule to the substrate (oxidation).

To distinguish between initial and final state effects, combined photoemission and X ray excited Auger electron spectroscopy (XAES) can be applied.^{36,78,80–83} The basic idea is that different final states in XPS (one hole) and XAES (two holes) cause different shifts in binding energy (E_B). For the analysis of these shifts often the change of the modified Auger parameter α' is monitored according to $\Delta\alpha' = \Delta E_B(\text{XPS}) + \Delta E_{\text{kin}}(\text{XAES})$ (E_{kin} corresponds to the kinetic energy), which is correlated to the dynamical or one hole relaxation energy R_D ($\Delta\alpha' \approx 2\Delta R_D$).^{79,80,84} ΔR_D can be correlated to the change of the polarization energy induced by the redistribution of environmental charges. The extra atomic relaxation energy R_D^{ca} is determined in macroscopic dielectric models by the

polarization charge $(1 - 1/\epsilon)e$, where ϵ is the optical dielectric constant of the environment.

For fluorinated Pcs the absence of a local charge transfer process at the fluorine atom allows the estimation of the polarization screening via the corresponding Auger parameter.³⁶ In addition, in contrast to C KVV and N KVV Auger spectra, F KLL Auger spectra include deeper valence levels (shallow core levels), resulting in comparably well resolved spectra. This allows a determination of the modified fluorine Auger parameter with an accuracy of about ± 0.15 eV. For a discussion of the shape of F KLL Auger spectra we refer to the literature.^{85,86}

We note that fluorinated phthalocyanines might be bended upon adsorption on metal surfaces. For submonolayers of CuPcF₁₆ on Cu(111) it was reported that fluorine atoms reside 0.027 nm above the benzene rings, which would result in an underestimation of the relaxation energy for carbon and nitrogen atoms. However, the effect is in the range of about 0.1 eV (cf. ref 36) and does not influence not the discussion below.

In Figure 9, we compare the development of the modified Auger parameter α' during the film growth of CoPcF₁₆ on Cu(110) and Cu(110) (2 × 1)O. The corresponding F 1s and F KLL spectra are shown in Figures S5 and S6. Because of the mirror charge screening effect of the metallic substrate, the

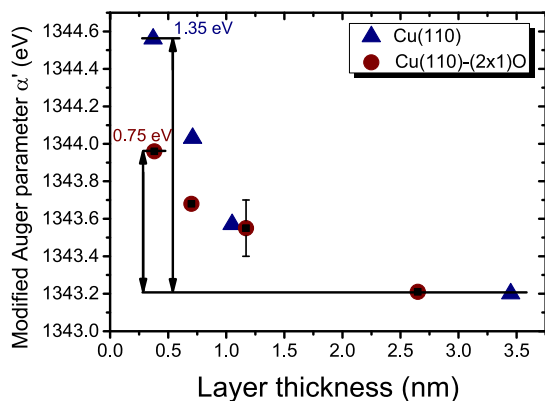


Figure 9. Modified Auger parameter α' for fluorine in CoPcF₁₆ as a function of film thickness of CoPcF₁₆ on Cu(110) and Cu(110) (2 × 1)O. The modified Auger parameter α' is calculated from the binding energy of the F 1s core level and the kinetic energy of the related F KLL. An accuracy of ± 0.15 eV is estimated.

highest value of α' in Figure 9 is found at monolayer coverages, that is, for molecules directly at the interface, where the screening ability is highest. Comparing the thickest films with monolayer coverages, changes of α' are 1.35 and 0.75 eV for CoPcF₁₆/Cu(110) and CoPcF₁₆/Cu(110) (2 × 1)O, respectively. The higher value for $\Delta\alpha'$ on Cu(110) can be well understood by the closer distance of CoPcF₁₆ molecules to the metallic mirror plane compared to the oxygen terminated surface.^{81,87} We mention that rather similar (higher or lower) values $\Delta\alpha'$ of 1.5 and 0.7 eV were obtained on the interfaces CoPcF₁₆/graphene/Ni(111) and CoPcF₁₆/Au(111),^{26,88} respectively, which were attributed to either stronger or weaker interacting interfaces. This similarity even extends to the Co 2p spectra and the apparent contributions of the interface peaks as discussed above.

Values for the relaxation energy contribution ΔR_D estimated from $\Delta\alpha'$ (Figure 9) are 0.7 and 0.4 eV for CoPcF₁₆ on Cu(110) and Cu(110) (2 × 1)O, respectively. This implies that shifts of photoemission core level spectra to lower binding

energies in the same order of magnitude might be expected as a function of the film thickness. Whereas shifts of C 1s and N 1s spectra of 0.2–0.3 eV are visible for CoPcF₁₆ on Cu(110) (2 × 1)O, on Cu(110) thickness dependent shifts are almost negligible (cf. Figures 1 and 2). Thus, we are left with the scenario that screening related shifts to lower binding energies, at least on Cu(110), are compensated to a large extent by another effect: a charge transfer from the macrocycle to the substrate at the very interface.

The complex charge transfer at both interfaces affects the valence band spectra, shown in Figure 10 as a function of the thickness. At about 3 nm CoPcF₁₆ film thickness, a single HOMO feature is visible in the spectra recorded from both surfaces; the energetic position (energy level alignment) is slightly different by 0.12 eV for the two surfaces (cf. Figure 8). This might be caused by the different interaction strength or energy level alignment of the first CoPcF₁₆ layer on both substrates. Clearly visible in the spectra is the formation of interface states (or a splitting of the HOMO) for low coverages. Such interface states may arise from a partial filling of the LUMO of the molecule as a consequence of the charge transfer,⁸⁹ or stronger changes of the electronic structure, such as the formation of new states due to hybridization between Co d orbitals and substrate related states, as proposed for other CoPcF₁₆/metal interfaces.^{19,53} From the XA spectra (cf. Figure 6), we conclude that a hybridization occurs at both investigated interfaces. On the other hand, the shapes of monolayer valence band spectra are somewhat different for the two substrates (features A, B, and C). We ascribe these variations to the different electronic interactions involved at the respective interfaces, rather likely related to different contributions of interacting molecules of the first layer on both substrates as well as to different involvement of the macrocycle in the interaction. Feature B, only visible for CoPcF₁₆ on Cu(110), might be related to the interaction between the macrocycle and the substrate.

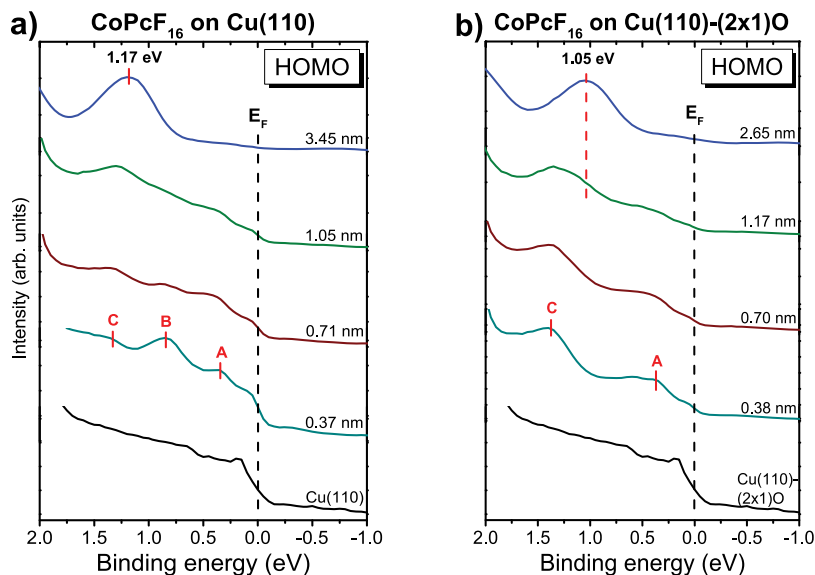


Figure 10. Thickness dependent valence band spectra (zoom into the HOMO region) of CoPcF₁₆ on (a) Cu(110) and (b) Cu(110) (2 × 1)O. Measured with an excitation energy of $h\nu = 21.22$ eV.

4. CONCLUSIONS

We studied interface properties of CoPcF₁₆ on Cu(110) and Cu(110) (2 × 1)O. In both cases, a charge transfer from the substrate to the central Co ion of CoPcF₁₆ is observed, even if the oxygen termination suppresses such a strong interaction for a part of the molecules of the first monolayer. The absence of such an interaction for FePcF₁₆ on Cu(110) (2 × 1)O indicates that the interfacial interaction in the case of CoPcF₁₆ is governed by a local interaction between the Co 3d_{z²} orbital and states of the substrate, similar to many CoPc and CoPcF₁₆ interfaces to noble metals.^{5,19,20} Considering the geometry of the Cu(110) (2 × 1)O surface, the interaction occurs most likely between the Co ion of CoPcF₁₆ and atoms of Cu–O rows of the added row reconstruction. Thus, this study demonstrates the special nature of the Co ion in Co phthalocyanines and related compounds.

Analyzing the energetic shifts of all core levels, distinguishing between screening of the photohole and initial state effects, we propose that the charge transfer between CoPcF₁₆ and Cu(110) is bidirectional, involving also the macrocycle of CoPcF₁₆. The conclusion is supported by analysis of the shape of N K XA spectra as a function of the thickness. It is demonstrated that the application of the Auger parameter concept is a very useful tool for the estimation of polarization screening contributions in binding energy shifts of core level photoemission spectra.

■ AUTHOR INFORMATION

Corresponding Author

Heiko Peisert – Institute of Physical and Theoretical Chemistry, University of Tübingen, 72076 Tübingen, Germany; orcid.org/0000-0002-9742-5800; Phone: (+49) 07071/29 76931; Email: heiko.peisert@uni-tuebingen.de; Fax: (+49) 07071/29 5490

Authors

Axel Belser – Institute of Physical and Theoretical Chemistry, University of Tübingen, 72076 Tübingen, Germany

Katharina Greulich – Institute of Physical and Theoretical Chemistry, University of Tübingen, 72076 Tübingen, Germany

Peter Grüniger – Institute of Physical and Theoretical Chemistry, University of Tübingen, 72076 Tübingen, Germany

Reimer Karstens – Institute of Physical and Theoretical Chemistry, University of Tübingen, 72076 Tübingen, Germany

Ruslan Ovsyannikov – Institute for Methods and Instrumentation in Synchrotron Radiation Research, Helmholtz Zentrum Berlin für Materialien und Energie GmbH, 12489 Berlin, Germany

Erika Giangrisostomi – Institute for Methods and Instrumentation in Synchrotron Radiation Research, Helmholtz Zentrum Berlin für Materialien und Energie GmbH, 12489 Berlin, Germany

Peter Nagel – Institute for Quantum Materials and Technologies (IQMT), Karlsruher Institut für Technologie, 76021 Karlsruhe, Germany

Michael Merz – Institute for Quantum Materials and Technologies (IQMT), Karlsruher Institut für Technologie, 76021 Karlsruhe, Germany

Stefan Schuppler – Institute for Quantum Materials and Technologies (IQMT), Karlsruher Institut für Technologie, 76021 Karlsruhe, Germany

Thomas Chassé – Institute of Physical and Theoretical Chemistry, University of Tübingen, 72076 Tübingen, Germany; Center for Light–Matter Interaction, Sensors & Analytics (LISA+) at the University of Tübingen, 72076 Tübingen, Germany; orcid.org/0000-0001-6442-8944

Notes

The authors declare no competing financial interest.

■ ACKNOWLEDGMENTS

The authors thank the Helmholtz Zentrum Berlin (electron storage ring BESSY II) for provision of synchrotron radiation at the beamline PM4. Financial travel support by HZB is thankfully acknowledged. The authors are grateful to the synchrotron light source KARA and to KNMF, both Karlsruhe, Germany, for the provision of beamtime. The Center for Light–Matter Interaction, Sensors & Analytics (LISA+) at the University of Tübingen is acknowledged for technical support.

■ REFERENCES

- (1) Koch, N. Organic Electronic Devices and Their Functional Interfaces. *ChemPhysChem* **2007**, *8*, 1438–1455.
- (2) Ma, H.; Yip, H. L.; Huang, F.; Jen, A. K. Y. Interface Engineering for Organic Electronics. *Adv. Funct. Mater.* **2010**, *20*, 1371–1388.
- (3) Sanvito, S. Molecular Spintronics. *Chem. Soc. Rev.* **2011**, *40*, 3336–3355.
- (4) Uihlein, J.; Polek, M.; Glaser, M.; Adler, H.; Ovsyannikov, R.; Bauer, M.; Ivanovic, M.; Preobrajenski, A. B.; Generalov, A. V.; Chassé, T.; et al. Influence of Graphene on Charge Transfer between CoPc and Metals: The Role of Graphene–Substrate Coupling. *J. Phys. Chem. C* **2015**, *119*, 15240–15247.
- (5) Balle, D.; Adler, H.; Grüniger, P.; Karstens, R.; Ovsyannikov, R.; Giangrisostomi, E.; Chassé, T.; Peisert, H. Influence of the Fluorination of CoPc on the Interfacial Electronic Structure of the Coordinated Metal Ion. *J. Phys. Chem. C* **2017**, *121*, 18564–18574.
- (6) Ameri, T.; Li, N.; Brabec, C. J. Highly Efficient Organic Tandem Solar Cells: A Follow up Review. *Energy Environ. Sci.* **2013**, *6*, 2390–2413.
- (7) Chung, K.; Lee, C. H.; Yi, G. C. Transferable Gan Layers Grown on ZnO Coated Graphene Layers for Optoelectronic Devices. *Science* **2010**, *330*, 655–657.

- (8) Kawasaki, T.; Ichimura, T.; Kishimoto, H.; Akbar, A. A.; Ogawa, T.; Oshima, C. Double Atomic Layers of Graphene/Monolayer H BN on Ni(111) Studied by Scanning Tunneling Microscopy and Scanning Tunneling Spectroscopy. *Surf. Rev. Lett.* **2002**, *09*, 1459–1464.
- (9) Scarfato, A.; Chang, S. H.; Kuck, S.; Brede, J.; Hoffmann, G.; Wiesendanger, R. Scanning Tunneling Microscope Study of Iron(II) Phthalocyanine Growth on Metals and Insulating Surfaces. *Surf. Sci.* **2008**, *602*, 677–683.
- (10) Ferretti, A.; Baldacchini, C.; Calzolari, A.; Di Felice, R.; Ruini, A.; Molinari, E.; Betti, M. G. Mixing of Electronic States in Pentacene Adsorption on Copper. *Phys. Rev. Lett.* **2007**, *99*, 046802.
- (11) Baldacchini, C.; Allegretti, F.; Gunnella, R.; Betti, M. G. Molecule Metal Interaction of Pentacene on Copper Vicinal Surfaces. *Surf. Sci.* **2007**, *601*, 2603–2606.
- (12) Koch, N.; Gerlach, A.; Duhm, S.; Glowatzki, H.; Heimel, G.; Vollmer, A.; Sakamoto, Y.; Suzuki, T.; Zegenhagen, J.; Rabe, J. P.; et al. Adsorption Induced Intramolecular Dipole: Correlating Molecular Conformation and Interface Electronic Structure. *J. Am. Chem. Soc.* **2008**, *130*, 7300–7304.
- (13) Müller, K.; Seitsonen, A. P.; Brugger, T.; Westover, J.; Greber, T.; Jung, T.; Kara, A. Electronic Structure of an Organic/Metal Interface: Pentacene/Cu(110). *J. Phys. Chem. C* **2012**, *116*, 23465–23471.
- (14) Ules, T.; Lüftner, D.; Reinisch, E. M.; Koller, G.; Puschnig, P.; Ramsey, M. G. Orbital Tomography of Hybridized and Dispersing Molecular Overlayers. *Phys. Rev. B: Condens. Matter Mater. Phys.* **2014**, *90*, 8.
- (15) Belser, A.; Karstens, R.; Nagel, P.; Merz, M.; Schuppler, S.; Chassé, T.; Peisert, H. Interaction Channels between Perfluorinated Iron Phthalocyanine and Cu(111). *Phys. Status Solidi B* **2019**, *256*, 1800292.
- (16) Tsukahara, N.; Noto, K. I.; Ohara, M.; Shiraki, S.; Takagi, N.; Takata, Y.; Miyawaki, J.; Taguchi, M.; Chainani, A.; Shin, S.; et al. Adsorption Induced Switching of Magnetic Anisotropy in a Single Iron(II) Phthalocyanine Molecule on an Oxidized Cu(110) Surface. *Phys. Rev. Lett.* **2009**, *102*, 167203.
- (17) Shen, K. C.; Narsu, B.; Ji, G. W.; Sun, H. L.; Hu, J. B.; Liang, Z. F.; Gao, X. Y.; Li, H. Y.; Li, Z. S.; Song, B.; et al. On Surface Manipulation of Atom Substitution between Cobalt Phthalocyanine and the Cu(111) Substrate. *RSC Adv.* **2017**, *7*, 13827–13835.
- (18) Grüninger, P.; Greulich, K.; Karstens, R.; Belser, A.; Ovsyannikov, R.; Giangrisostomi, E.; Bettinger, H. F.; Batchelor, D.; Peisert, H.; Chassé, T. Highly Oriented Hexacene Molecules Grown in Thin Films on Cu(110) (2×1)O. *J. Phys. Chem. C* **2019**, *123*, 27672–27680.
- (19) Ruckerl, F.; Waas, D.; Buchner, B.; Knupfer, M. Particular Electronic Properties of F₁₆CoPc: A Decent Electron Acceptor Material. *J. Electron Spectrosc. Relat. Phenom.* **2017**, *215*, 1–7.
- (20) Peisert, H.; Uihlein, J.; Petraki, F.; Chassé, T. Charge Transfer between Transition Metal Phthalocyanines and Metal Substrates: The Role of the Transition Metal. *J. Electron Spectrosc. Relat. Phenom.* **2015**, *204*, 49–60.
- (21) Guo, J.; Li, H.; He, H.; Chu, D.; Chen, R. CoPc and CoPcF₁₆ Modified Ag Nanoparticles as Novel Catalysts with Tunable Oxygen Reduction Activity in Alkaline Media. *J. Phys. Chem. C* **2011**, *115*, 8494–8502.
- (22) Baran, J. D.; Larsson, J. A.; Woolley, R. A. J.; Cong, Y.; Moriarty, P. J.; Cafolla, A. A.; Schulte, K.; Dhanak, V. R. Theoretical and Experimental Comparison of Snpc, Pbpc, and CoPc Adsorption on Ag(111). *Phys. Rev. B: Condens. Matter Mater. Phys.* **2010**, *81*, 075413.
- (23) Yeh, J. J.; Lindau, I. Atomic Subshell Photoionization Cross Sections and Asymmetry Parameters: $1 \leq Z \leq 103$. *At. Data Nucl. Data Tables* **1985**, *32*, 1–155.
- (24) Hesse, R.; Chassé, T.; Streubel, P.; Szargan, R. Error Estimation in Peak Shape Analysis of XPS Core Level Spectra Using Unifit 2003: How Significant Are the Results of Peak Fits? *Surf. Interface Anal.* **2004**, *36*, 1373–1383.
- (25) Horcas, I.; Fernández, R.; Gómez Rodríguez, J. M.; Colchero, J.; Gómez Herrero, J.; Baro, A. M. WSXM: A software for scanning probe microscopy and a tool for nanotechnology. *Rev. Sci. Instrum.* **2007**, *78*, 013705.
- (26) Petraki, F.; Peisert, H.; Uihlein, J.; Aygül, U.; Chassé, T. CoPc and CoPcF₁₆ on Gold: Site Specific Charge Transfer Processes. *Beilstein J. Nanotechnol.* **2014**, *5*, 524–531.
- (27) Lindner, S.; Treske, U.; Knupfer, M. The Complex Nature of Phthalocyanine/Gold Interfaces. *Appl. Surf. Sci.* **2013**, *267*, 62–65.
- (28) Huang, Y.; Wruss, E.; Egger, D.; Kera, S.; Ueno, N.; Saidi, W.; Bucko, T.; Wee, A.; Zojer, E. Understanding the Adsorption of CuPc and ZnPc on Noble Metal Surfaces by Combining Quantum Mechanical Modelling and Photoelectron Spectroscopy. *Molecules* **2014**, *19*, 2969–2992.
- (29) Jiang, H.; Ye, J.; Hu, P.; Wei, F.; Du, K.; Wang, N.; Ba, T.; Feng, S.; Kloc, C. Fluorination of Metal Phthalocyanines: Single Crystal Growth, Efficient N Channel Organic Field Effect Transistors, and Structure Property Relationships. *Sci. Rep.* **2015**, *4*, 7573.
- (30) Peisert, H.; Knupfer, M.; Schwieger, T.; Fuentes, G. G.; Olligs, D.; Fink, J.; Schmidt, T. Fluorination of Copper Phthalocyanines: Electronic Structure and Interface Properties. *J. Appl. Phys.* **2003**, *93*, 9683–9692.
- (31) Wang, J.; Wang, J.; Dougherty, D. B. Direct Molecular Quantification of Electronic Disorder in N,N' Di [(1 Naphthyl) N,N' Diphenyl] 1,1' Biphenyl) 4,4' Diamine on Au(111). *J. Vac. Sci. Technol., B: Nanotechnol. Microelectron.: Mater., Process., Meas., Phenom.* **2020**, *38*, 053401.
- (32) Peisert, H.; Knupfer, M.; Fink, J. Energy Level Alignment at Organic/Metal Interfaces: Dipole and Ionization Potential. *Appl. Phys. Lett.* **2002**, *81*, 2400–2402.
- (33) Vazquez, H.; Dappe, Y. J.; Ortega, J.; Flores, F. Energy Level Alignment at Metal/Organic Semiconductor Interfaces: “Pillow” Effect, Induced Density of Interface States, and Charge Neutrality Level. *J. Chem. Phys.* **2007**, *126*, 144703.
- (34) Betti, M. G.; Kanjilal, A.; Mariani, C.; Vázquez, H.; Dappe, Y. J.; Ortega, J.; Flores, F. Barrier Formation at Organic Interfaces in a Cu(100) Benzenethiolate Pentacene Heterostructure. *Phys. Rev. Lett.* **2008**, *100*, 027601.
- (35) Yamane, H.; Yoshimura, D.; Kawabe, E.; Sumii, R.; Kanai, K.; Ouchi, Y.; Ueno, N.; Seki, K. Electronic Structure at Highly Ordered Organic/Metal Interfaces: Pentacene on Cu(110). *Phys. Rev. B: Condens. Matter Mater. Phys.* **2007**, *76*, 165436.
- (36) Peisert, H.; Kolacyak, D.; Chassé, T. Site Specific Charge Transfer Screening at Organic/Metal Interfaces. *J. Phys. Chem. C* **2009**, *113*, 19244–19250.
- (37) Evangelista, F.; Ruocco, A.; Gotter, R.; Cossaro, A.; Floreano, L.; Morgante, A.; Crispoldi, F.; Betti, M. G.; Mariani, C. Electronic States of CuPc Chains on the Au(110) Surface. *J. Chem. Phys.* **2009**, *131*, 174710.
- (38) Papageorgiou, N.; Ferro, Y.; Salomon, E.; Allouche, A.; Layet, J. M.; Giovanelli, L.; Le Lay, G. Geometry and Electronic Structure of Lead Phthalocyanine: Quantum Calculations Via Density Functional Theory and Photoemission Measurements. *Phys. Rev. B: Condens. Matter Mater. Phys.* **2003**, *68*, 235105.
- (39) Papageorgiou, N.; Salomon, E.; Angot, T.; Layet, J. M.; Giovanelli, L.; Lay, G. L. Physics of Ultra Thin Phthalocyanine Films on Semiconductors. *Prog. Surf. Sci.* **2004**, *77*, 139–170.
- (40) Schmid, M.; Kaftan, A.; Steinrück, H. P.; Gottfried, J. M. The Electronic Structure of Cobalt(II) Phthalocyanine Adsorbed on Ag(111). *Surf. Sci.* **2012**, *606*, 945–949.
- (41) Maslyuk, V. V.; Aristov, V. Y.; Molodtsova, O. V.; Vyalikh, D. V.; Zhilin, V. M.; Ossipyan, Y. A.; Bredow, T.; Mertig, I.; Knupfer, M. The Electronic Structure of Cobalt Phthalocyanine. *Appl. Phys. A: Mater. Sci. Process.* **2009**, *94*, 485–489.
- (42) Åhlund, J.; Nilson, K.; Schiessling, J.; Kjeldgaard, L.; Berner, S.; Mårtensson, N.; Puglia, C.; Brena, B.; Nyberg, M.; Luo, Y. The Electronic Structure of Iron Phthalocyanine Probed by Photoelectron and X Ray Absorption Spectroscopies and Density Functional Theory Calculations. *J. Chem. Phys.* **2006**, *125*, 034709.

- (43) Willey, T. M.; Bagge Hansen, M.; Lee, J. R.; Call, R.; Landt, L.; van Buuren, T.; Colesniuc, C.; Monton, C.; Valmianski, I.; Schuller, I. K. Electronic Structure Differences between H_2 , Fe, Co, and Cu Phthalocyanine Highly Oriented Thin Films Observed Using NEXAFS Spectroscopy. *J. Chem. Phys.* **2013**, *139*, 034701.
- (44) Holland, B. N.; Peltakis, N.; Farrelly, T.; Wilks, R. G.; Gavrilu, G.; Zahn, D. R. T.; McGuinness, C.; McGovern, I. T. NEXAFS Studies of Copper Phthalocyanine on Ge(001) 2×1 and Ge(111) $c(2 \times 8)$ Surfaces. *Phys. Status Solidi B* **2009**, *246*, 1546–1551.
- (45) Petraki, F.; Peisert, H.; Hoffmann, P.; Uihlein, J.; Knupfer, M.; Chassé, T. Modification of the 3d Electronic Configuration of Manganese Phthalocyanine at the Interface to Gold. *J. Phys. Chem. C* **2012**, *116*, 5121–5127.
- (46) Kuz'min, M. D.; Hayn, R.; Oison, V. Ab Initio Calculated XANES and XMCD Spectra of Fe(II) Phthalocyanine. *Phys. Rev. B: Condens. Matter Mater. Phys.* **2009**, *79*, 024413.
- (47) Betti, M. G.; Gargiani, P.; Frisenda, R.; Biagi, R.; Cossaro, A.; Verdini, A.; Floreano, L.; Mariani, C. Localized and Dispersive Electronic States at Ordered FePc and CoPc Chains on Au(110). *J. Phys. Chem. C* **2010**, *114*, 21638–21644.
- (48) Bartolomé, J.; Bartolomé, F.; Garcia, L. M.; Filoti, G.; Gredig, T.; Colesniuc, C. N.; Schuller, I. K.; Cezar, J. C. Highly Unquenched Orbital Moment in Textured Fe Phthalocyanine Thin Films. *Phys. Rev. B: Condens. Matter Mater. Phys.* **2010**, *81*, 195405.
- (49) Javaid, S.; Bowen, M.; Boukari, S.; Joly, L.; Beaufrand, J. B.; Chen, X.; Dappe, Y. J.; Scheurer, F.; Kappler, J. P.; Arabski, J.; et al. Impact on Interface Spin Polarization of Molecular Bonding to Metallic Surfaces. *Phys. Rev. Lett.* **2010**, *105*, 077201.
- (50) Petraki, F.; Peisert, H.; Ayyul, U.; Latteyer, F.; Uihlein, J.; Vollmer, A.; Chassé, T. Electronic Structure of FePc and Interface Properties on Ag(111) and Au(100). *J. Phys. Chem. C* **2012**, *116*, 11110–11116.
- (51) Karstens, R.; Glaser, M.; Belsler, A.; Balle, D.; Polek, M.; Ovsyannikov, R.; Giangrisostomi, E.; Chassé, T.; Peisert, H. FePc and FePcF₁₆ on Rutile TiO₂(110) and (100): Influence of the Substrate Preparation on the Interaction Strength. *Molecules* **2019**, *24*, 4579.
- (52) Toader, M.; Gopakumar, T. G.; Shukryna, P.; Hietschold, M. Exploring the F₁₆CoPc/Ag(110) Interface Using Scanning Tunneling Microscopy and Spectroscopy. 2. Adsorption Induced Charge Transfer Effect. *J. Phys. Chem. C* **2010**, *114*, 21548–21554.
- (53) Lindner, S.; Treske, U.; Grobosch, M.; Knupfer, M. Charge Transfer at F₁₆CoPc and CoPc Interfaces to Au. *Appl. Phys. A: Mater. Sci. Process.* **2011**, *105*, 921–925.
- (54) Petraki, F.; Peisert, H.; Biswas, I.; Chassé, T. Electronic Structure of Co Phthalocyanine on Gold Investigated by Photoexcited Electron Spectroscopies: Indication of Co Ion Metal Interaction. *J. Phys. Chem. C* **2010**, *114*, 17638–17643.
- (55) Toader, M.; Knupfer, M.; Zahn, D. R. T.; Hietschold, M. Initial Growth at the F₁₆CoPc/Ag(111) Interface. *Surf. Sci.* **2011**, *605*, 1510–1515.
- (56) Pawlak, R.; Meier, T.; Renaud, N.; Kisiel, M.; Hinaut, A.; Glatzel, T.; Sordes, D.; Durand, C.; Soe, W. H.; Baratoff, A.; et al. Design and Characterization of an Electrically Powered Single Molecule on Gold. *ACS Nano* **2017**, *11*, 9930–9940.
- (57) Lindner, S.; Mahns, B.; Treske, U.; Vilkov, O.; Haidu, F.; Fronk, M.; Zahn, D. R. T.; Knupfer, M. Epitaxial Growth and Electronic Properties of Well Ordered Phthalocyanine Heterojunctions MnPc/F₁₆CoPc. *J. Chem. Phys.* **2014**, *141*, 094706.
- (58) Fernández Rodríguez, J.; Toby, B.; van Veenendaal, M. Mixed Configuration Ground State in Iron(II) Phthalocyanine. *Phys. Rev. B: Condens. Matter Mater. Phys.* **2015**, *91*, 214427.
- (59) Uihlein, J.; Peisert, H.; Glaser, M.; Polek, M.; Adler, H.; Petraki, F.; Ovsyannikov, R.; Bauer, M.; Chassé, T. Communication: Influence of Graphene Interlayers on the Interaction between Cobalt Phthalocyanine and Ni(111). *J. Chem. Phys.* **2013**, *138*, 081101.
- (60) Coulman, D. J.; Wintterlin, J.; Behm, R. J.; Ertl, G. Novel Mechanism for the Formation of Chemisorption Phases: The (2×1) O Cu(110) “Added Row” Reconstruction. *Phys. Rev. Lett.* **1990**, *64*, 1761–1764.
- (61) Jensen, F.; Besenbacher, F.; Laegsgaard, E.; Stensgaard, I. Surface Reconstruction of Cu(110) Induced by Oxygen Chemisorption. *Phys. Rev. B: Condens. Matter Mater. Phys.* **1990**, *41*, 10233–10236.
- (62) Duan, X.; Warschkow, O.; Soon, A.; Delley, B.; Stampfl, C. Density Functional Study of Oxygen on Cu(100) and Cu(110) Surfaces. *Phys. Rev. B: Condens. Matter Mater. Phys.* **2010**, *81*, 15.
- (63) Stepanow, S.; Miedema, P. S.; Mugarza, A.; Ceballos, G.; Moras, P.; Cezar, J. C.; Carbone, C.; de Groot, F. M. F.; Gambardella, P. Mixed Valence Behavior and Strong Correlation Effects of Metal Phthalocyanines Adsorbed on Metals. *Phys. Rev. B: Condens. Matter Mater. Phys.* **2011**, *83*, 220401.
- (64) Li, Z.; Li, B.; Yang, J.; Hou, J. G. Single Molecule Chemistry of Metal Phthalocyanine on Noble Metal Surfaces. *Acc. Chem. Res.* **2010**, *43*, 954–962.
- (65) Bai, Y.; Sekita, M.; Schmid, M.; Bischof, T.; Steinruck, H. P.; Gottfried, J. M. Interfacial Coordination Interactions Studied on Cobalt Octaethylporphyrin and Cobalt Tetraphenylporphyrin Mono layers on Au(111). *Phys. Chem. Chem. Phys.* **2010**, *12*, 4336–4344.
- (66) Lukaszczuk, T.; Flechtner, K.; Merte, L. R.; Jux, N.; Maier, F.; Gottfried, J. M.; Steinruck, H. P. Interaction of Cobalt(II) Tetraarylporphyrins with a Ag(111) Surface Studied with Photoelectron Spectroscopy. *J. Phys. Chem. C* **2007**, *111*, 3090–3098.
- (67) Hieringer, W.; Flechtner, K.; Kretschmann, A.; Seufert, K.; Auwärter, W.; Barth, J. V.; Görling, A.; Steinrück, H. P.; Gottfried, J. M. The Surface Trans Effect: Influence of Axial Ligands on the Surface Chemical Bonds of Adsorbed Metalloporphyrins. *J. Am. Chem. Soc.* **2011**, *133*, 6206–6222.
- (68) Greulich, K.; Belsler, A.; Bölke, S.; Grüninger, P.; Karstens, R.; Sättele, M. S.; Ovsyannikov, R.; Giangrisostomi, E.; Basova, T. V.; Klyamer, D.; et al. Charge Transfer from Organic Molecules to Molybdenum Disulfide: Influence of the Fluorination of Iron Phthalocyanine. *J. Phys. Chem. C* **2020**, *124*, 16990–16999.
- (69) Kroll, T.; Kraus, R.; Schonfelder, R.; Aristov, V. Y.; Molodtsova, O. V.; Hoffmann, P.; Knupfer, M. Transition Metal Phthalocyanines: Insight into the Electronic Structure from Soft X Ray Spectroscopy. *J. Chem. Phys.* **2012**, *137*, 054306.
- (70) Nakamura, K.; Kitaoka, Y.; Akiyama, T.; Ito, T.; Weinert, M.; Freeman, A. J. Constraint Density Functional Calculations for Multiplets in a Ligand Field Applied to Fe Phthalocyanine. *Phys. Rev. B: Condens. Matter Mater. Phys.* **2012**, *85*, 235129.
- (71) Dale, B. W.; Williams, R. J. P.; Johnson, C. E.; Thorp, T. L. S = 1 Spin State of Divalent Iron. I. Magnetic Properties of Phthalocyanine Iron (II). *J. Chem. Phys.* **1968**, *49*, 3441–3444.
- (72) Natoli, C. R.; Kruger, P.; Bartolome, J.; Bartolome, F. Determination of the Ground State of an Au Supported FePc Film Based on the Interpretation of Fe K and L Edge X Ray Magnetic Circular Dichroism Measurements. *Phys. Rev. B: Condens. Matter Mater. Phys.* **2018**, *97*, 16.
- (73) Ivanco, J.; Haber, T.; Krenn, J. R.; Netzer, F. P.; Resel, R.; Ramsey, M. G. Sexithiophene Films on Ordered and Disordered TiO₂ Surfaces: Electronic, Structural and Morphological Properties. *Surf. Sci.* **2007**, *601*, 178–187.
- (74) Duhm, S.; Heimel, G.; Salzmann, I.; Glowatzki, H.; Johnson, R. L.; Vollmer, A.; Rabe, J. P.; Koch, N. Orientation Dependent Ionization Energies and Interface Dipoles in Ordered Molecular Assemblies. *Nat. Mater.* **2008**, *7*, 326–332.
- (75) Ishii, H.; Sugiyama, K.; Ito, E.; Seki, K. Energy Level Alignment and Interfacial Electronic Structures at Organic/Metal and Organic/Organic Interfaces. *Adv. Mater.* **1999**, *11*, 605–625.
- (76) Hwang, J.; Wan, A.; Kahn, A. Energetics of Metal Organic Interfaces: New Experiments and Assessment of the Field. *Mater. Sci. Eng., R* **2009**, *64*, 1–31.
- (77) Crispin, X.; Geskin, V.; Crispin, A.; Cornil, J.; Lazzaroni, R.; Salaneck, W. R.; Brédas, J. L. Characterization of the Interface Dipole at Organic/ Metal Interfaces. *J. Am. Chem. Soc.* **2002**, *124*, 8131–8141.

- (78) Kaindl, G.; Chiang, T. C.; Eastman, D. E.; Himpsel, F. J. Distance Dependent Relaxation Shifts of Photoemission and Auger Energies for Xe on Pd(001). *Phys. Rev. Lett.* **1980**, *45*, 1808–1811.
- (79) Peisert, H.; Chassé, T.; Streubel, P.; Meisel, A.; Szargan, R. Relaxation Energies in XPS and XAES of Solid Sulfur Compounds. *J. Electron Spectrosc. Relat. Phenom.* **1994**, *68*, 321–328.
- (80) Moretti, G. The Wagner Plot and the Auger Parameter as Tools to Separate Initial and Final State Contributions in X Ray Photo emission Spectroscopy. *Surf. Sci.* **2013**, *618*, 3–11.
- (81) Kolacyak, D.; Peisert, H.; Chassé, T. Charge Transfer and Polarization Screening in Organic Thin Films: Phthalocyanines on Au(100). *Appl. Phys. A: Mater. Sci. Process.* **2009**, *95*, 173–178.
- (82) Chiang, T. C.; Kaindl, G.; Mandel, T. Layer Resolved Shifts of Photoemission and Auger Spectra from Physisorbed Rare Gas Multilayers. *Phys. Rev. B: Condens. Matter Mater. Phys.* **1986**, *33*, 695–711.
- (83) Peisert, H.; Petershans, A.; Chassé, T. Charge Transfer and Polarization Screening at Organic/Metal Interfaces: Distinguishing between the First Layer and Thin Films. *J. Phys. Chem. C* **2008**, *112*, 5703–5706.
- (84) Moretti, G. The Auger Parameter and the Polarization Energy a Simple Electrostatic Model. *Surf. Interface Anal.* **1990**, *16*, 159–162.
- (85) Albridge, R. G.; Hamrin, K.; Johansson, G.; Fahlman, A. The KLL Auger Spectrum of Fluorine. *Z. Phys. A: Hadrons Nucl.* **1968**, *209*, 419–427.
- (86) Vékey, K. Multiply Charged Ions. *Mass Spectrom. Rev.* **1995**, *14*, 195–225.
- (87) Helander, M. G.; Greiner, M. T.; Wang, Z. B.; Lu, Z. H. Effect of Electrostatic Screening on Apparent Shifts in Photoemission Spectra near Metal/Organic Interfaces. *Phys. Rev. B: Condens. Matter Mater. Phys.* **2010**, *81*, 153308.
- (88) Balle, D.; Schedel, C.; Chassé, T.; Peisert, H. Interface Properties of CoPc and CoPcF₁₆ on Graphene/Nickel: Influence of Germanium Intercalation. *J. Phys.: Condens. Matter* **2019**, *31*, 174004.
- (89) Schwieger, T.; Peisert, H.; Knupfer, M. Direct Observation of Interfacial Charge Transfer from Silver to Organic Semiconductors. *Chem. Phys. Lett.* **2004**, *384*, 197–202.